AIP | Applied Physics Letters

Single-quantum-well grating-gated terahertz plasmon detectors

E. A. Shaner, Mark Lee, M. C. Wanke, A. D. Grine, J. L. Reno et al.

Citation: Appl. Phys. Lett. **87**, 193507 (2005); doi: 10.1063/1.2128057
View online: http://dx.doi.org/10.1063/1.2128057
View Table of Contents: http://apl.aip.org/resource/1/APPLAB/v87/i19
Published by the American Institute of Physics.

Single-quantum-well grating-gated terahertz plasmon detectors

E. A. Shaner,[a] Mark Lee, M. C. Wanke, A. D. Grine, and J. L. Reno
Sandia National Laboratories, P.O. Box 5800, Albuquerque, New Mexico 87185

S. J. Allen
Center for Terahertz Science and Technology, University of California at Santa Barbara, Santa Barbara, California 93106

(Received 29 June 2005; accepted 12 September 2005; published online 2 November 2005)

A grating-gated field-effect transistor fabricated from a *single*-quantum well in a high-mobility GaAs–AlGaAs heterostructure is shown to function as a continuously electrically tunable photodetector of terahertz radiation via excitation of resonant plasmon modes in the well. Different harmonics of the plasmon wave vector are mapped, showing different branches of the dispersion relation. As a function of temperature, the resonant response magnitude peaks at around 30 K. Both photovoltaic and photoconductive responses have been observed under different incident power and bias conditions. © *2005 American Institute of Physics*. [DOI: 10.1063/1.2128057]

The terahertz (THz) frequency dynamics of high-mobility field-effect transistors (FETs) are largely controlled by collective charge density oscillations, or plasmons, of the two-dimensional electron gas (2DEG) in the FET channel. This has led to a great deal of recent interest in exploiting two-dimensional (2D) plasmons for very high-frequency electronics. Most immediate applications have centered on detection and generation of THz frequency electromagnetic radiation.[1] Changes in temperature alter the strength and width of these 2D plasmon resonances through changes in electron mobility and the amplitude of the spatial density modulation in the device.[2] Typical electron densities of 10^{10} to 10^{12} cm^{-2} and device geometries of several microns in high-mobility 2DEG systems lead to plasmon modes in the ~1 THz range.[3] A most attractive feature emerges from the fact that the electron density and hence the 2D plasmon resonance frequencies are readily tuned by an applied gate voltage bias. By gating and controlling 2D plasmons, a tunable THz detector has emerged. Electrical tunability provides an important functionality unavailable in nearly all existing THz detection technologies.

Recent explorations of plasmon resonant THz detectors have used single-layer 2DEGs in III-V semiconductor and $Si-SiO_2$ heterostructures as direct detectors at fixed frequency.[4–6] III-V semiconductor double-quantum-well (DQW) heterostructures have demonstrated direct detection[7] and mixing[8] in a continuously gate-tunable FET. In the previous work, it was amply clear that the detector response resonated with the 2D plasmon, but a physical mechanism that produces changes in conductance or source-drain voltage has not emerged.[9] In fact, Ref. 7 speculated that a DQW channel was important.

This letter shows that a single-quantum-well device behaves in a very similar way. *Thus, the DQW is not essential to the development of sensitive, fast, and tunable plasmon THz detectors*. We report the first experimental demonstration of a continuously tunable THz detection in a *single*-quantum-well detector and document its dependence on incident frequency, wave vector harmonics, and temperature. Furthermore, unlike the previous work which showed primarily photoconductive response,[7] we observe here a THz plasmon response dominated by a photovoltaic response.

The dispersion relation for 2D plasmon resonances in a heterostructure FET is given by

$$f_0^2 = \frac{1}{4\pi^2}\frac{e^2 n(V_G) k_j}{2\varepsilon\varepsilon_0 m^*}, \tag{1}$$

where f_0 is the resonance frequency, e is the electron charge, $n(V_G)$ is the 2DEG density at a gate bias V_G, $k_j = jk_1$ is the jth harmonic mode of the plasmon wave vector ($j=1,2,3,\ldots$), $\varepsilon\varepsilon_0$ is the dielectric constant of the semiconductor, and m^* is the effective electron mass.[10] For the THz detectors discussed here, the lowest wave vector $k_1 = 2\pi/4$ μm is fixed by the 4 μm period of the grating gate, (2 μm metal +2 μm gap) and corresponds to one-half of a plasmon wavelength fitting underneath the gate metal line.

From Eq. (1), for a single incident THz frequency, resonance may occur at different densities for different spatial harmonics k_j. Thus, there may be multiple plasmon resonances available in the device at different carrier densities or gate biases. Furthermore, at a particular plasmon mode j the square of the resonant frequency should be linearly dependent on carrier density alone.

The grating-gated FETs are fabricated from a single-modulation-doped GaAs–AlGaAs quantum well (QW), 40 nm wide, formed 200 nm below the wafer surface. The QW has approximate electron density of 2.5×10^{11} cm^{-2} and mobility $\mu \approx 5\times10^6$ cm^2/V s. The device is fabricated on an isolation mesa etched completely though the 2DEG. Standard annealed Ohmic contacts form the source and drain. The grating gate is comprised of 20 nm Ti and 50 nm Au and has a 4 μm, 50% duty cycle period over a 2 mm$\times$2 mm area. When this gate is biased with respect to the underlying QW, it creates a nonuniform spatially modulated carrier density. Under these conditions, the coupling to resonant plasmon modes produces an electrical photoresponse that displays a rich spectrum of behavior depending on incident power, plasmon mode index, and source-drain bias current.

Measurements were made using two distinct THz sources that overlapped in frequency but permitted a wide range of power: (1) A continuous wave (cw) molecular gas far-infrared laser, and (2) a widely tunable pulsed free-

[a]Electronic mail: eashane@sandia.gov

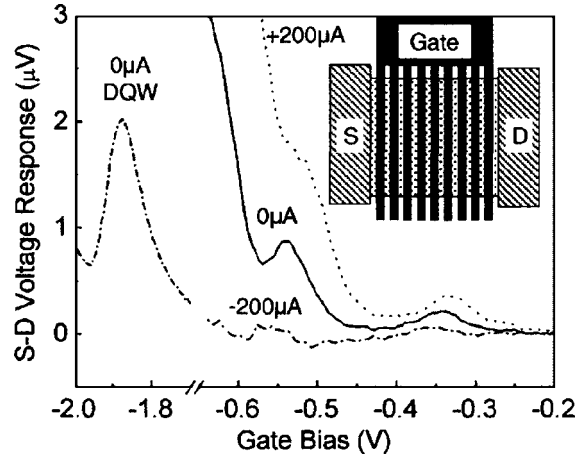

FIG. 1. Photoresponse of single QW and DQW detectors. The single-well data span from −0.2 to −0.65 V and are shown at three different source-drain currents. The double-well detector is shown from −1.6 to −2.2 V at $I_{SD}=0$. Measurements were taken using a cw source at 763 GHz. In this setup, with a few mW incident power, there is a clear PV signal present at $I_{SD}=0$ for both types of detectors.

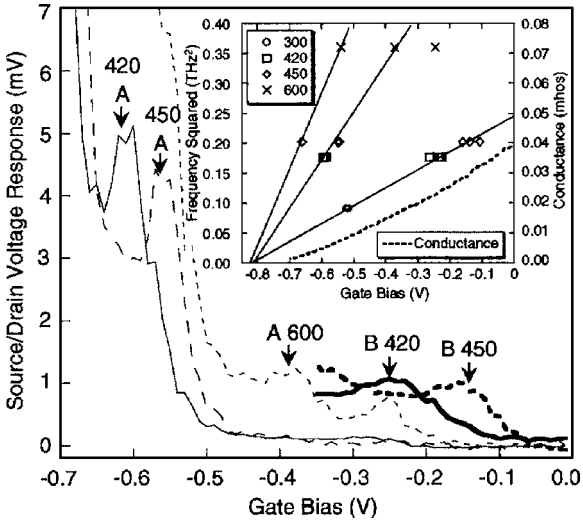

FIG. 2. Photoresponse at different wavelengths using $I_{SD}=100$ μA. The inset shows peak position vs V_G from a larger set of FEL data. Lines drawn through the peak points extrapolate back to near the conductance pinchoff voltage.

electron laser (FEL). The electrical response measurement was essentially identical in both cases. A bias current (I_{SD}) was applied between the source and drain with the drain grounded, while a gate voltage bias (V_G) was applied with respect to the drain. Additional source and drain leads were used for signal detection in a quasi-four point arrangement. In the cw case, the signal leads were fed into a lock-in amplifier referenced to a 390 Hz chopping frequency. For the FEL measurements, the signal leads were buffered by a differential amplifier before being read by a high-speed digitizing oscilloscope.

Figure 1 shows the $T=20$ K device cw photoresponse versus V_G at three different I_{SD} using 763 GHz illumination. Clear peaks are observed around $V_G=-0.32$ V and −0.53 V, corresponding to two plasmon modes at this one frequency. The dc pinchoff voltage, V_P, is near −0.75 V. As V_G approaches V_P, the response magnitude is seen to increase as previously observed in DQW grating gate detectors.[7] One interesting feature of these data is the large resonant signal when $I_{SD}=0$, indicating a mostly photovoltaic (PV) response. For $I_{SD}=+200$ μA, the PV signal peaks shift slightly to the right. The peak shifting is consistent with a gradient in effective gate bias due to the source-drain voltage drop. For $I_{SD}=-200$ μA, the resonant response remains positive-going, again indicating a mostly PV response. In previous DQW detector work, the primary response was observed to be mostly photoconductive (PC).[7] In contrast, under the measurement conditions used here, the photoresponse of a DQW device shown in Fig. 1 at $I_{SD}=0$ is photovoltaic. This PV behavior of both single- and double-well detectors under the same experimental conditions has been consistently observed. Overall, this leads us to believe that both single- and double-well responses are based on the same physical mechanisms.

The observation of the large, broadband PV response close to V_P also prompts a re-evaluation of the physical processes responsible. It was previously proposed that this pinchoff behavior in a DQW detector arises from a bolometric mechanism,[8] a conclusion based on the broadband character of the response and on the very similar behavior of the responsivity and the temperature slope of the source-drain resistance, dR_{SD}/dT, both as a function of V_G near 4 K. However, a strictly bolometric response cannot give rise to a PV signal. Examining Eq. (1), the number of modes per change in electron density increases rapidly as the gated carrier density approaches zero at V_P. This compression of mode spacing and the consequent overlap of higher-order peaks as $V_G \rightarrow V_P$ allows for the excitation of many closely spaced plasmon modes for any frequency and may explain the broadband response and increasing responsivity near pinchoff. Since each low-order mode has demonstrated a PV response in the single-well detectors, a superposition of multiple simultaneously excited higher-order modes may also explain the pinch-off PV response observed. The previous correlation of the response tracking dR_{SD}/dT may be coincidental, but it is possible that the pinchoff response could well be a combination of both bolometric and higher-mode excitation effects, with relative contributions depending on temperature, bias conditions, and illumination power.

The frequency and power dependencies were investigated with the FEL, which provided 2 μs pulses with peak power of approximately 1 kW that were strongly attenuated before being focused directly onto the sample. A software boxcar technique sampled the peak signal height of the photoresponse. This peak is the signal amplitude in Fig. 2 which shows the photoresponse (for $I_{SD}=100$ μA) at two different power attenuation levels: *A* (−36 dB attenuation) and *B* (−16 dB attenuation).[11] Three frequencies, 420, 450, and 600 GHz, were characterized at Power *A*. In Fig. 2, arrows mark plasmon modes having the largest response. At Power *B* (420 and 450 GHz shown), the peaks found at Power *A* between −0.5 V to −0.6 V are smeared out (data truncated for clarity). In both cases, as the frequency is increased, the resonant peaks shift toward $V_G=0$ (i.e., higher density) in accordance with Eq. (1). Over the range of attenuations used (10 dB to 55 dB) varying amounts of PV and PC contributions to the photoresponse were observed.

Figure 2 inset plots observed resonant peak V_G versus square of illumination frequency at 300, 420, 450, and 600 GHz over all the power ranges measured using $I_{SD}=+100$ μA. With the exception of one 600 GHz peak near

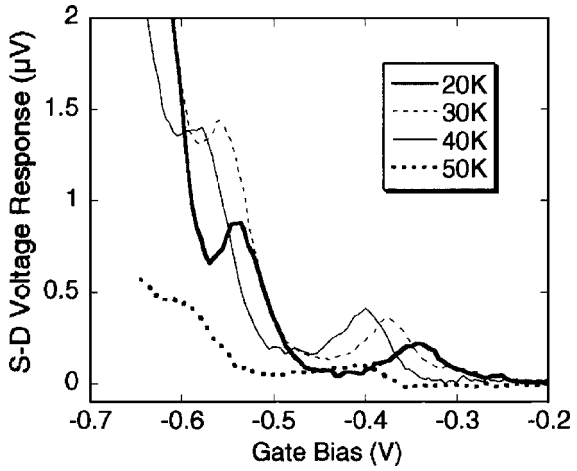

FIG. 3. Temperature dependence of PV response. As T increases from 20 K, the resonant peaks shift closer to pinchoff. The responsivity of the peak between −0.35 V and −0.45 V peaks between 30 K and 40 K and then rapidly falls off as T was increased further.

−0.25 V gate bias, the data fall onto three separate lines which all intersect at zero frequency at $V_G=-0.80$ V, nearly the same as the dc conductance pinchoff voltage $V_P=-0.75$ V. These linear dependencies and extrapolation to zero frequency at pinchoff follow very well the plasmon dispersion form of Eq. (1) if we take $n\propto(V_G-V_P)$. Empirically, the slopes of the three lines in Fig. 2 have the ratio 1: 2.8: 4.6, which is close to the 1:3:5 ratio expected from Eq. (1) for the $j=1$, 3, and 5 modes. Extrapolating the lowest mode to zero gate bias yields an ungated plasma frequency of 490 GHz. This is only a 15% discrepancy with the 425 GHz plasma frequency of the ungated $j=1$ mode calculated from Eq. (1), providing an independent check on our assignment of mode number.

Similar to the DQW plasmon detectors originally investigated, these single-well detectors show a responsivity maximum at elevated temperatures. Figure 3 shows the response of a single-well detector at 763 GHz in the cw setup from $T=20$ to 50 K. The data were measured with $I_{SD}=0$ (i.e., PV response), but other currents showed similar temperature behavior. As T is increased from 20 K, the resonance near −0.35 V shifts toward pinchoff. The responsivity of this mode peaks between 30 and 40 K before dying off at 50 K. It is difficult to describe the behavior of the mode near −0.55 V as the temperature change shifts its position into the pinchoff regime. The mechanism behind this unusual temperature dependence is not presently understood.

Grating-gate FETs fabricated from single-quantum material have been found to produce plasmon related photoresponse similar to those previously found in DQW devices. Single-well devices have many advantages compared to double-well structures, such as lower biasing requirements and easier fabrication of other on-chip electronics for amplification. The photovoltaic signal observed, if it can be understood, could possibly be enhanced and harnessed in order to create detectors that operate without a bias current. Such devices could be beneficial for imaging arrays where reducing the dissipated chip power would be an advantage. Further investigation of the nonlinear plasmon dynamics involved in these processes, along with improvements in device design, should lead to an increase in the device responsivity.

Sandia is a multiprogram laboratory operated by Sandia Corporation, a Lockheed–Martin Company, for the United States Department of Energy's National Nuclear Security Administration under Contract No. DE-AC04-94AL85000. Work at UCSB is supported by the ARO.

[1] X. Peralta and W. Knap, Int. J. High Speed Electron. Syst. **12**, 491 (2002).
[2] M. Dyakonov and M. S. Shur, in *Terahertz Sources and Systems*, edited by R. E. Miles (Kluwer Academic, Netherlands, 2001), pp. 187–207.
[3] S. J. Allen, D. C. Tsui, and R. A. Logan, Phys. Rev. Lett. **38**, 980 (1977); D. C. Tsui, E. Gornik, and R. A. Logan, Solid State Commun. **5**, 875 (1980).
[4] W. Knap, Y. Deng, S. Rumyantsev, J.-Q. Lu, M. S. Shur, C. A. Saylor, and L. C. Brunel, Appl. Phys. Lett. **80**, 3433 (2002); W. Knap, Y. Deng, S. Rumyantsev, M. S. Shur, *ibid.* **81**, 4637 (2002).
[5] W. Knap, F. Teppe, Y. Meziani, N. Dyakonova, J. Lusakowski, F. Boeuf, T. Skotnicki, D. Maude, S. Rumyantsev, and M. S. Shur, Appl. Phys. Lett. **85**, 675 (2004).
[6] T. Otsuji, M. Hanabe, and O. Ogawara, Appl. Phys. Lett. **85**, 2119 (2004).
[7] X. G. Peralta, S. J. Allen, M. C. Wanke, N. E. Harff, J. A. Simmons, M. P. Lilly, J. L. Reno, P. J. Burke, and J. P. Eisenstein, Appl. Phys. Lett. **81**, 1627 (2002).
[8] M. Lee, M. C. Wanke, and J. L. Reno, Appl. Phys. Lett. **86**, 033501 (2005).
[9] V. V. Popov, O. V. Polischuk, T. V. Teperik, X. G. Peralta, S. J. Allen, N. J. M. Horing, and M. C. Wanke, J. Appl. Phys. **94**, 3556 (2003).
[10] The grating metallization alters this dispersion relation, especially at small wavevectors. This can be modeled by an effective dielectric constant $\varepsilon(\kappa)$. This is not essential to the discussion or interpretation here.
[11] Typical FEL output power is approximately 1 kW. While attenuation levels were calibrated at each frequency, the actual power levels reaching the sample were not measured. While not precise, the ratio between power levels A and B is reasonably accurate, and is the relevant information for understanding the data presented in Fig. 2